Technical Report No. 32-76

Rapid-Rate Compression Testing of Sheet Materials at High Temperatures

E. C. Bernett

W. W. Gerberich

jpl

JET PROPULSION LABORATORY
CALIFORNIA INSTITUTE OF TECHNOLOGY
PASADENA, CALIFORNIA

June 15, 1961

Technical Report No. 32-76

Rapid-Rate Compression Testing of Sheet Materials at High Temperatures

E. C. Bernett

W. W. Gerberich

L. D. Jaffe, Chief
Materials Research

JET PROPULSION LABORATORY
CALIFORNIA INSTITUTE OF TECHNOLOGY
PASADENA, CALIFORNIA

June 15, 1961

CONTENTS

TABLES

FIGURES

ABSTRACT

This Report describes the test equipment that was developed and the procedures that were used to evaluate structural sheet-material compression properties at preselected constant strain rates and/or loads. Electrical self-resistance was used to achieve a rapid heating rate of 200°F/sec. Four materials were tested at maximum temperatures which ranged from 600°F for the aluminum alloy to 2000°F for the Ni-Cr-Co iron-base alloy. Tests at 0.1, 0.001, and 0.00001 in./in./sec showed that strain rate has a major effect on the measured strength, especially at the high temperatures. The tests, under conditions of constant temperature and constant compression stress, showed that creep deformation can be a critical factor even when the time involved is on the order of a few seconds or less. The theoretical and practical aspects of rapid-rate compression testing are presented, and suggestions are made regarding possible modifications of the equipment which would improve the over-all capabilities.

I. COMPRESSION TESTING PROGRAM

A. Introduction

The spectacular success of air-breathing jet engines and, more recently, the modern rocket devices is due in large measure to the development of special structural materials capable of withstanding the extremely high operating temperatures and stresses. It goes without saying that the design engineers working on these devices have done excellent work despite many major handicaps. For example, where components must operate for some given length of time while subject to both high temperatures and high stresses, the design problems are often nearly impossible to resolve analytically. In many instances the failure of the analytical approach is directly due to lack of sufficient mechanical property data for the possible candidate materials under the specific service conditions. In these cases, therefore, new designs and development work are often based on "last year's experience."

Where high temperatures are encountered in aeronautical or space-vehicle applications, the design problems are even more formidable, because the over-all weight must be kept to a minimum. The science of designing for elevated-temperature service has received a great deal of attention during the last twenty years and will get even more in the future. It is not the purpose here to discuss the various aspects of this subject, as these are being adequately covered in the current literature.

Reference is made to one special case only; that is, the short-time or transient condition of high temperature and high stress in structural components. Under such conditions, major gains can be made with regard to designing for minimum weight if suitable short-time elevated-temperature test data are available. The purpose of this Report is to describe the equipment and techniques used for determining specialized data of this nature. Specifically, these data are rapid-rate compression stress–strain

behavior and short-time compression creep properties of sheet materials at temperatures ranging into the 2000°F region. Some of the theoretical considerations involved in such tests are discussed, and suggestions are made regarding methods of extending the capabilities of this testing technique.

B. Test Equipment

The compression tests described in this Report were carried out on an automatically controlled test machine developed by the Marquardt Corporation specifically for rapid-rate testing of aircraft structural materials. Details regarding physical layout, capacities, operating capabilities, accuracies, and other features may be found in Ref. 1. Essentially, the machine is an hydraulically operated horizontal type with a capacity of 50,000-lb tension or compression. The maximum ram speed possible is 0.75 in./sec. Constant preselected testing speeds (strain rate or load rate, whichever is preferred) are maintained automatically by means of electrical feedback in the control circuitry. Load-versus-strain data are recorded on a fast-response X-Y plotter. The fastest speed at which accurate and sufficiently magnified load-versus-strain curves can be recorded is on the order of 0.2 in./in./sec strain rate. In the case of elevated-temperature tests, the specimens are heated by electrical self-resistance. Temperatures are measured and controlled through thermocouples spot-welded directly to the test portion of the specimen.

The compression tests were carried out on double pin-type flat specimens with an ASTM standard gage section (Fig. 1). This specimen is exactly the same as the tensile specimens used for the subject test machine. This is advantageous from a number of standpoints. First, the specimens provide a generous gripping surface. Thus, good electrical contact is obtained, and the possibility of overheating in this area is eliminated. Second, the large gripping surface helps to distribute the applied compres-

sion loads more uniformly. Thus, the possibility of local deformation at the loading points (which could cause eccentric loading) is minimized. Third, the double pin-type specimen configuration assures positive alignment for each test. Fourth, the compression specimens could be machined with the same tooling and fit the same test-machine adapters as those used for the tension specimens. This results in lower fabrication costs and reduces the setup time on the test machine.

The lateral support fixture used in these tests is illustrated schematically in Figs. 2 and 3. Photographs of this unit installed on the test machine are shown in Ref. 1. Essentially, the fixture consists of two rigid stainless-steel stiffeners (top and bottom support in Fig. 2) which clamp on either side of the sheet-metal specimen. The supports are tied to the bed of the test machine by means of cantilevered braces and an angle plate. The braces were designed in the illustrated fashion in order to accommodate the compressometer in the space directly below the test specimen.

Figure 2. Front view of lateral support fixture

A simple method of aligning the lateral supports was incorporated into the design of this equipment. It may be noted in Fig. 3 that the bolt-down holes in the braces are slotted (vertically). For any test series, the first specimen was centered in the test machine and the bottom support located flush with the underside of the test section and then bolted tightly to the angle plate. The top support could then be lowered onto the specimen, snugged up by finger-tightening the cross link, and then it, too, was bolted securely to the angle plate. The top support could be removed and replaced when changing specimens, and no readjustment would be necessary as long as the gage of the specimens being tested remained

Figure 1. Sheet-metal compression test specimen

2

Figure 3. Side view of lateral support fixture

highly desirable from the standpoint of minimizing the frictional loads generated between the specimen and the lateral supports.

As mentioned previously, the compressometer was located in the space directly below the test specimen. The linkage arms extended upward and were clamped to the sides of the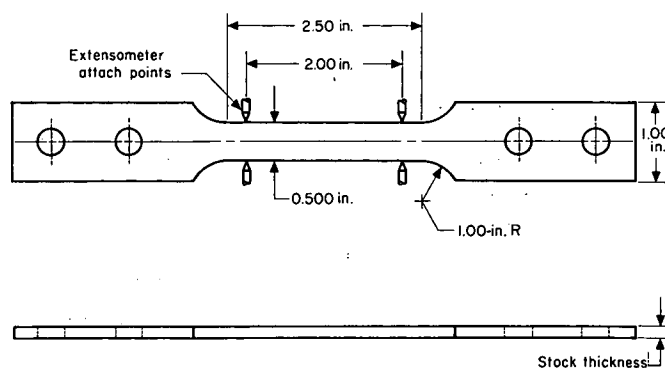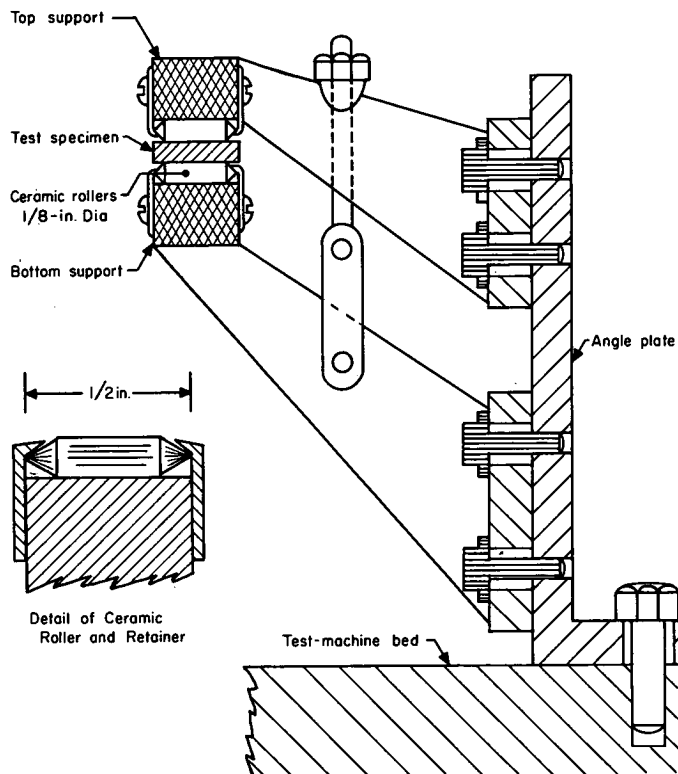 test specimen at the points shown in Fig. 1. The contact points were the same grade of alumina ceramic as was used for the lateral support rollers. The ceramic contact points provided electrical insulation between the specimen and the strain sensor and also minimized the heat drain at the points where contact was made with the specimen. It might also be pointed out that by locating the compressometer as indicated above, a major difficulty often encountered in rapid-state testing was eliminated. The case in point is that thermal expansion of the extensometer linkage arms during a test can result in erroneous strain readout. In the extensometer system used here, the linkage arms extend out at 90 deg to the longitudinal axis of the test specimen. Heating of the arms is minimized, and, furthermore, any slight arm growth that may occur has no detectable effect on the indicated strain.

The measurement and control of temperature under conditions of rapid heating (e.g., 200°F/sec) presents a number of problems. This is especially true in the case of compression tests where portions of the specimen test section are in contact with the lateral support fixture. Chromel–alumel thermocouples made from 0.005-in.-diameter wire were spot-welded along the exposed edge of the specimen. Direct measurement of the temperature along the flats (i.e., the portions of the specimen in contact with the lateral supports) could not be made using conventional methods because of the close quarters involved. Series of elevated-temperature tensile tests were therefore run with and without the compression fixtures installed. The measured values were equivalent; thus, it was concluded that the temperature-measuring technique was accurate. A further check on the accuracy of the indicated temperatures was made by comparing the measured tension and compression Young's Modulus values. Within the limits of experimental error, these values were equivalent at all check points.

the same. Frequent checks were made to ensure that the bottom support remained solidly bolted.

As indicated previously, self-resistance heating was used in this test program. It was necessary, therefore, to provide both electrical and thermal insulation between the specimen and the steel lateral supports. Commercial alumina ceramic rollers (0.125-in. diameter × 0.500-in. length, 60-deg point both ends) were, therefore, used along the working faces of the top and bottom support. Stainless-steel retainers were bolted along the front and back and at both ends of the lateral supports to keep the ceramic rollers in place. In order to minimize brinelling, the working faces of the supports were surface-hardened by flame-spraying to a depth of approximately 0.030 in.

It may be observed in Fig. 2 that the ceramic rollers extend almost the entire 4-in. length of the lateral supports. With regard to the test specimen, the rollers span the full 2.5-in. parallel test portion as well as the radiused areas. During setup of each specimen, care was taken to ensure that the rollers were positioned as shown in Fig. 2. That is, the rollers were all pushed together tightly in the direction of the movable crosshead of the test machine. This resulted in a space at the far ends of the lateral supports, and when the compression test was started the rollers could roll in the direction of straining. This is

C. Test Program and Results

The sheet materials evaluated on the subject equipment to date include bare 2024-T81 aluminum alloy, 17-7 PH(TH1050) stainless steel, 6Al-4V titanium alloy, and a 20Cr-20Ni-20Co iron-base alloy (N-155). The aluminum sheet was 0.125 in. thick, and the other three materials were 0.070 gage. The test temperatures ranged up to

600°F for the aluminum, up to 1400°F for the stainless and titanium, and up to 2000°F for the N-155 alloy. The rate of heating to the test temperature was a nominal 200°F/sec. Two hold times at temperature (i.e., 2 and 30 min) were evaluated. It was desired to check the effect of testing speed on the compression properties; therefore, three widely different strain rates, i.e., 0.00001, 0.001, and 0.1 in./in./sec, were used. The compression-stress versus strain curves obtained under the above-described condi-

tions were recorded automatically on a rapid-rate *X-Y* plotter. At least two, and in some cases as many as five, replicate tests were carried out in order that the data-scatter bands could be more closely defined. A complete listing of individual test results and the derived typical curves of compression strength, compression modulus, and tangent modulus is given in Ref. 1. Summary tabulations of these data are shown in Tables 1 through 3, inclusive.

Table 1. Typical compression proportional-limit strengths of aircraft-type structural materials

Temperature °F	Bare 2024-T81 aluminum sheet			17-7PH (TH 1050) stainless sheet			Annealed 6Al-4V titanium sheet			Annealed N-155 alloy sheet		
	Strain rate											
	Low	Med	High	Low	Med	High	Low	Med	High	Low	Med	High
75	57.5	57.5	57.5	166	166	166	127	127	127	16.2	16.2	16.2
200	54.0	54.4	54.6	163	163	163	106	106	106	15.8	15.8	15.8
400	36.5	42.0	44.5	155	156	157	87	87	87	15.1	15.1	15.1
600	10.0	18.0	24.0	133	141	145	77	77	77	14.5	14.5	14.5
800				90	110	121	64	68	69	14.0	14.0	14.0
1000				32	55	84	36	51	60	13.5	13.5	13.5
1200				8	22	46	8	26	48	13.1	13.1	13.1
1400				2	14	27		11	35	12.9	12.9	12.9
1600										9.0	12.6	12.6
1800										3.9	10.5	11.1
2000										1.5	5.4	9.1

Notes:
1. Strain rates, in./in./sec: low = 0.00001, medium = 0.001, high = 0.1.
2. Specimens heated by electrical self-resistance at 200°F/sec.
3. Hold time at temperature: 2 min for aluminum, 2 and 30 min all others.

Table 2. Typical 0.2% compression yield strengths of aircraft-type structural materials

Temperature °F	Bare 2024-T81 aluminum sheet			17-7PH (TH 1050) stainless sheet			Annealed 6Al-4V titanium sheet			Annealed N-155 alloy sheet		
	Strain rate											
	Low	Med	High	Low	Med	High	Low	Med	High	Low	Med	High
75	71.5	71.5	71.5	200	208	213	131	137	139	43.0	43.0	43.0
200	66.5	67.0	67.5	198	205	211	109	115	121	37.0	37.0	37.0
400	44.8	51.5	57.0	188	197	204	90	96	102	31.2	31.2	31.2
600	15.0	24.0	34.0	167	180	188	79	87	91	29.0	29.0	29.0
800				121	147	162	68	77	82	28.4	28.4	28.4
1000				51	92	120	45	65	73	28.0	28.0	28.0
1200				16	37	68	15	42	62	27.9	27.9	27.9
1400				5	21	46	4	18	50	27.4	27.7	27.7
1600										18.0	26.9	26.9
1800										7.5	17.0	21.9
2000										3.0	8.0	16.9

Notes:
1. Strain rates, in./in./sec: low = 0.00001, medium = 0.001, high = 0.1.
2. Specimens heated by electrical self-resistance at 200°F/sec.
3. Hold time at temperature: 2 min for aluminum, 2 and 30 min all others.

Table 3. Typical tension and compression modulus of aircraft-type structural materials

Temperature °F	Bare 2024-T81 aluminum sheet		17-7PH (TH 1050) stainless sheet		Annealed 6Al-4V titanium sheet		Annealed N-155 alloy sheet	
	Tension	Compression	Tension	Compression	Tension	Compression	Tension	Compression
75	10.3	10.6	28.0	29.1	15.9	15.9	30.0	30.2
200	9.9	10.3	27.6	28.7	15.5	15.5	29.0	29.2
400	9.2	9.4	26.6	27.7	14.7	14.7	27.4	27.5
600	7.9	8.5	25.2	26.4	13.8	13.7	25.7	25.9
800			23.2	24.3	12.7	12.7	23.9	24.0
1000			19.9	20.8	11.2	11.3	22.1	22.2
1200			15.0	15.8	8.9	9.0	20.3	20.3
1400			9.0	9.5	5.0	5.0	18.3	18.0
1600							16.0	15.6
1800							13.0	12.5
2000							9.0	8.6

Notes:
  1. Strain rates, in./in./sec: 0.001 and 0.1 for aluminum, 0.00001, 0.001, and 0.1 all others.
  2. Specimens heated by electrical self-resistance at 200°F/sec.
  3. Hold time at temperature: 2 and 30 min.

Constant-load tests (compression creep) were also carried out on the above-described materials in order to supplement the constant strain-rate data. The specimen configuration, the test setup, method of heating, and the heating rate were all exactly the same as those in the previous test series. The specimens were heated to the desired temperature, held for one minute, and then the required load was applied. Actually, a zero hold time at temperature was desired, but this is not practical because time is required for temperature-stabilization and for final pre-test adjustments of the equipment. The rate of loading to the desired creep stress was very rapid— essentially, at the full ram speed of 0.75 in./sec. This ram speed corresponds to a strain rate of approximately 0.1 in./in./sec. The constant applied load was held for a maximum time of 15 min or until the ram had travelled the full stroke of 0.125 in., whichever occurred first. The compression-creep strain versus time was recorded continuously on a fast strip-chart recorder.

The tests were run at three different temperatures for each material, and from two to five tests were run at each stress level in order to better establish the data-scatter bands. The individual test results are all listed in Ref. 1. To illustrate the general relationship between compression strengths measured at constant rate and those measured at constant stresses, a correlative plot of the referenced data is shown in Fig. 4. It is readily apparent that as the temperature increases, creep becomes more and more critical.
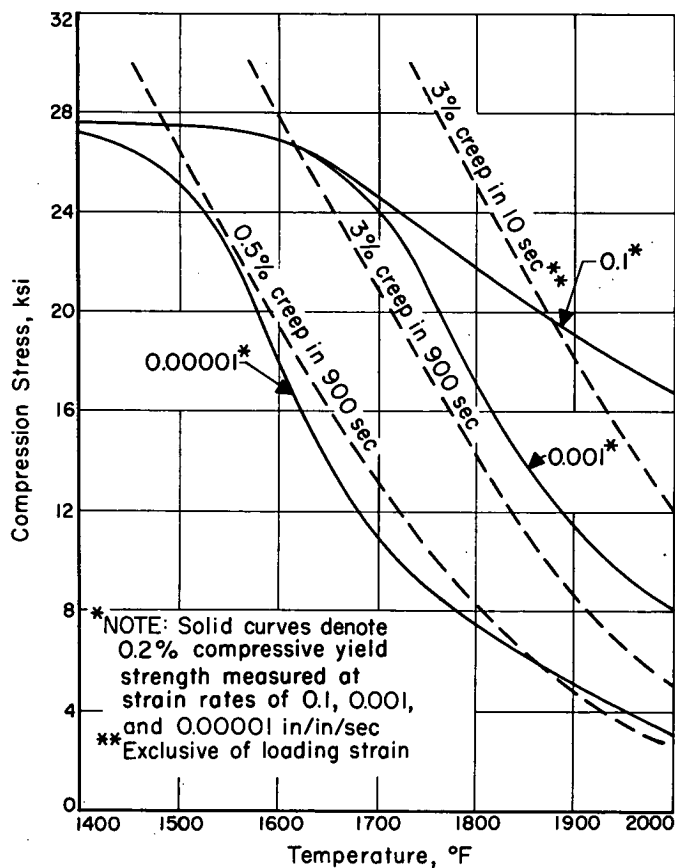

Figure 4. Compression-creep and compression-yield-strength curves for N-155 alloy sheet

II. ANALYSIS OF COMPRESSION LOADING

A. Theoretical Treatment

The geometrical loading condition used in this investigation is analogous to a large number of stiff springs supporting a long compression member. At buckling, the member buckles in rigid sections between supports. From the standard Euler formula, the critical wavelength l between supports for rectangular sections is

$$l = \left(\frac{\pi^2 E t^2}{12 \sigma_c} \right)^{1/2} \qquad (1)$$

where E is the modulus, t is the thickness and σ_c is the compressive stress. Since the major parameter of interest here is the compressive yield strength, further discussion will take E as the tangent modulus at the compressive yield strength and σ_c as the compressive yield strength. This is a reasonable approximation, as Shanley and others have shown that the tangent-modulus calculation compares favorably with experimental data in the plastic range.

From potential-energy, work, and equilibrium considerations, the lateral support load may be determined in terms of the deflection, the compressive load, and the wavelength. Furthermore, the deflection may be calculated in terms of the eccentricity, side load, and spring constant. It should be mentioned here that the eccentricity term consists of both the specimen-fixture misalignment and the slop between the side supports and the specimen. Assuming that a hinged-roller combination adequately describes the system at the yield strength, the lateral support load is determined to be

$$P_x = \frac{2\Delta_0 \dfrac{P_y}{l}}{1 - \dfrac{P_y}{P_{cr}}} \qquad (2)$$

where Δ_0 is the combined eccentricity term, P_y is the compressive load at the yield strength, and P_{cr} is the critical buckling load calculated from

$$P_{cr} = \frac{Kl}{4} \qquad (3)$$

A detailed derivation of these formulas is given in the Appendix. It is seen from Eqs. (2) and (3) that by making the spring constant K much larger than necessary, a built-in safety factor is provided for the system to the compressive yield strength.

Therefore, if it is assumed that K is sufficiently large, the critical factor for the magnitude of the side load is the eccentricity term. Utilizing the tangent modulus and 0.2% offset compressive-yield-strength data of this investigation, l may be calculated from Eq. (1). The critical buckling load is calculated from Eq. (3), using an arbitrary value of 200,000 lb/in. for the spring constant. Then, knowing P_y, P_{cr}, and l, the lateral support load may be calculated from Eq. (2) for various eccentricities. These calculations are shown in Table 4 for 2024-T81 aluminum and 17-7 PH (1050) stainless steel. Using these data, the ratio of lateral load to compressive load is plotted as a function of temperature for several eccentricities in Figs. 5 and 6. As long as the lateral load is less than about 3% of the compressive load, the friction force will probably have a small effect on the results. Within this limit, the 0.125-in.-thick aluminum alloy in Fig. 5 can withstand a relatively large eccentricity. However, for the thinner stainless-steel alloy in Fig. 6, little eccentricity can be tolerated.

B. Practical Considerations

The first consideration should be the effect of temperature on the validity of the results. As can be seen in Figs. 5 and 6, the ratio of the lateral load to the compressive load decreases with increasing temperature. In these cases, the results would probably be more accurate at the higher temperatures, other things being equal. The reason for this is that the ratio of the compressive yield strength to tangent modulus decreases with increasing temperature, as shown in Fig. 7. As long as this is the case, the effect of temperature on the validity of the results can be considered small.

In determining the minimum specimen thickness that can be tested, inter-roller buckling is the practical limitation. From Eq. (1), the minimum thickness t_{min} is determined from

$$t_{min} = \frac{l_{min}}{\pi} \left(\frac{12 \sigma_{cy}}{E_t} \right)^{1/2} \qquad (4)$$

where l_{min} is the inter-roller distance. In the equipment and in this investigation, l_{min} was 0.125 in. The minimum thickness is also dependent upon the maximum value of σ_{cy}/E_t, which occurs at room temperature (see Fig. 7). For the 2024-T81 aluminum alloy, this ratio is 5.56×10^{-2} and for the 17-7 PH stainless steel, it is 5.84×10^{-2}. Using a value of 6×10^{-2}, Eq. (4) gives t_{min} as approximately 0.034 in. Of ourse, being able to test this thickness without buckling is dependent upon the spring constant of the system.

Table 4. Calculation of lateral support load for various eccentricities

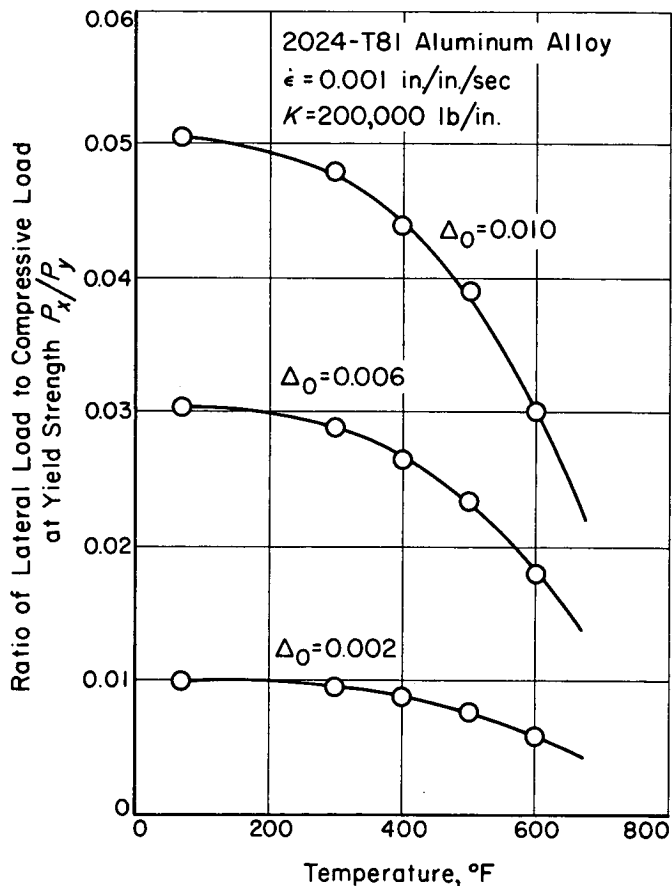| 2024-T81 aluminum sheet; 0.125-in. thick; $\dot{\varepsilon} = 0.001$ in./in./sec; $K = 200,000$ lb/in.											
Temperature °F	Modulus* $\times 10^6$ psi	σ_{cy} $\times 10^3$ psi	P_y lb	l in.	P_{cr} lb	$\Delta_0 = 0.002$ in.		$\Delta_0 = 0.006$ in.		$\Delta_0 = 0.010$ in.	
						P_x, lb	P_x/P_y	P_x, lb	P_x/P_y	P_x, lb	P_x/P_y
70	1.3	71.0	4440	0.484	24,200	44.9	0.0101	134.7	0.0303	222.5	0.0505
300	1.15	61.0	3820	0.494	24,700	36.6	0.0096	109.8	0.0288	183.0	0.0480
400	1.05	51.0	3180	0.516	25,800	28.0	0.0088	84.0	0.0264	140.0	0.0440
500	0.95	38.5	2400	0.560	28,000	18.8	0.0078	56.4	0.0234	94.0	0.0390
600	0.90	24.0	1500	0.693	34,600	9.04	0.0060	27.1	0.0180	45.2	0.0300
17-7 PH (TH 1050) stainless sheet; 0.072-in. thick; $\dot{\varepsilon} = 0.001$ in./in./sec; $K = 200,000$ lb/in.											
70	3.5	207	7530	0.268	13,400	256	0.0340	768	0.1020	1280	0.170
600	3.4	181	6510	0.280	14,000	174	0.0267	522	0.0801	870	0.133
800	3.2	147	5290	0.304	15,200	107	0.0202	321	0.0606	535	0.101
1000	2.6	91	3280	0.348	17,400	46.4	0.0141	129	0.0423	232	0.0705
1200	1.7	37	1330	0.442	22,100	12.8	0.0096	38.4	0.0288	64	0.0480
1400	1.4	20	720	0.545	27,200	5.43	0.0075	16.2	0.0225	26.5	0.0375

*E_t, tangent modulus at compressive yield strength.

Figure 5. Plots of lateral-to-compressive-load ratios
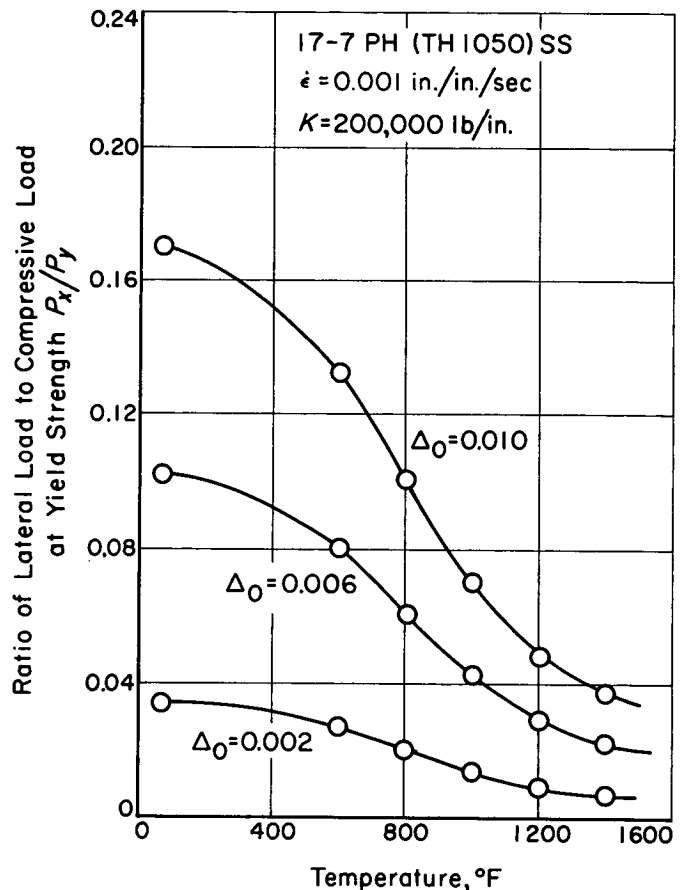for 2024-T81 aluminum

Figure 6. Plots of lateral-to-compressive-load ratios
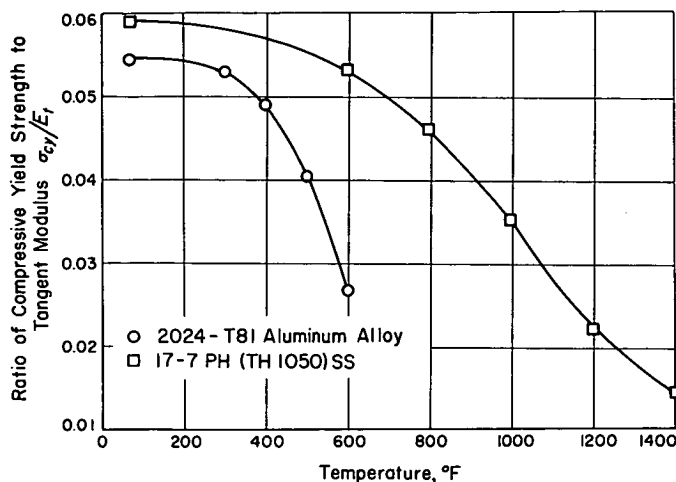for 17-7PH (TH 1050) stainless steel

Figure 7. Relationship of compressive yield strength and tangent modulus for 2024 aluminum and 17-7 stainless steel

The maximum allowable eccentricity may also be calculated for the most restrictive condition, which is the minimum wavelength of 0.125 in. Assuming that a lateral load of 3% of the compressive load is tolerable, $P_x/P_y = 0.03$. For a safety factor of two, $P_y/P_{cr} = 0.50$. The eccentricity Δ_0 is then calculated from Eq. (2) to be approximately 0.001 in. Thus, it is seen that for relatively thin specimens, the maximum allowable eccentricity is quite small.

As the previous discussion assumed that the testing fixture is rigid enough to provide a margin of safety against buckling, the last consideration will be the necessary spring constant of the system. For a safety factor of two, $K = 8P_y/l$. The wavelength may be calculated from Eq. (1), knowing the thickness and σ_{cy}/E_t. For example, say that the minimum thickness to be tested is 0.050 in. Using a σ_{cy}/E_t value of 6×10^{-2}, the wavelength is calculated to be 0.185 in. Since the member will buckle to points of contact with the side support, the wavelength would be a multiple of the inter-roller distance, in this case, 0.125 in. For a 250,000-psi yield-strength material and a 0.050 by 0.50-in. gage section, P_y is calculated to be 6250 lb. From these data, the spring constant of the system is found to be 400,000 lb/in. It is obvious that, for a reasonable margin of safety, an extremely rigid testing fixture is needed for moderately thin specimens.

The previous suggestions should be used only as guideposts to design and not as quantitative certainties. First of all, it is not certain how accurately the equations predict the state of the material at the yield strength. Secondly, values of the compressive yield strength and tangent modulus would not be accurately known before testing. Therefore, it is suggested that the lateral support have a high value of K and that a method be devised for measuring P_x during the test. One way would be to build a load cell into the lateral support. Unfortunately, this is impractical from two standpoints. First, for buckling in many waves, one would not know where to put the load cell to monitor P_x. Secondly, it would be difficult to obtain a load cell that would read small load values as well as being stiff enough for a 400,000-lb/in. spring system.

An alternative method would be to employ two load cells, one at either end of the specimen fixture. The difference between the two load-cell readings would represent the friction loss to the ceramic rollers. This system would have two advantages in that the effect of friction force on the results would immediately be known and that no special load cell would be needed. Its big disadvantage would be that P_x could not be very accurately determined, because the friction coefficients between ceramics and metals are not well defined.

In Ref. 2, coefficients of friction μ between magnetite (Fe_3O_4) and titanium, copper, aluminum, and zinc varied from 0.20 to 0.25. This and other data indicated that the friction coefficient for a metal–ceramic couple is relatively independent of the metal. Thus, for a particular type of ceramic roller, a single value of μ could be used for all data, and a relative value for P_x could be determined from

$$P_x = \frac{L_1 - L_2}{N\mu} \qquad (5)$$

where L_1 and L_2 are the load-cell readings and N is the number of points of contact on the side supports. A reasonable value for N may be calculated from Eq. (1). Then, if K and Δ_0 of the system can be measured, a reasonable check on the validity of Eqs. (1), (2), and (3) can be accomplished. Although the proper magnitude of P_x might not be determined, the trend of P_x with temperature, thickness, and eccentricity should be indicated.

III. CONCLUSIONS

1. The equipment developed and the test methods used are satisfactory for measuring the compression properties of structural sheet metals under conditions of rapid heating and loading. Maximum test temperatures of 2000°F were readily achieved. Tests up to the 3000°F range should be possible with no equipment modifications, and beyond this it would only be necessary to change lateral support-roller material to a high-melting-point ceramic.

2. The tests carried out in this program have shown that large differences in the measured compression strengths can be obtained by varying the testing speed. This behavior is quite analogous to that observed in tension tests.

3. At the upper useful temperature limits for any material, the time-dependent compression strength (i.e., creep strength) can become a governing design factor, even in those cases where the service time is on the order of a few seconds or less.

4. For the loading condition of this equipment, the theoretical relationship between side load, eccentricity, and wavelength is found to be

$$P_x = \frac{2\Delta_0 \dfrac{P_y}{l}}{1 - \dfrac{P_y}{P_{cr}}}$$

5. As long as the ratio of the compressive yield strength to tangent modulus decreases with increasing temperature, the effect of temperature on the validity of the results can be considered small.

6. The minimum thickness of specimens to be tested by this equipment is approximately 0.034 in., considering the spring constant of the system to be sufficiently large.

7. For relatively thin specimens, the maximum allowable eccentricity term is quite small, being about 0.001 in. for this equipment.

8. An extremely stiff lateral support system is needed to test relatively thin specimens. For a reasonable margin of safety, the spring constant must be on the order of 200,000 to 400,000 lb/in.

9. In order to check the validity of both the results and the theoretical treatment, it is recommended that two load cells be used to measure the compressive load, the difference between them representing the friction loss.

REFERENCES

1. Bernett, E. C., "Short Time Elevated Temperature Stress-Strain Behavior of Tensile, Compressive and Column Members," Wright Air Development Center, Technical Report 59-484 (December 1959).

2. Machlin, E. S., and Yankee, W. R., "Friction of Clean Metals and Oxides with Special Reference to Titanium," *Journal of Applied Physics*, Vol. 25, No. 5, May 1954, pp. 576–581.

APPENDIX

Calculation of Theoretical Relationship Between Lateral Support Load, Eccentricity, and Wavelength

If P_y is taken at the compressive yield strength,

$$P_y = \sigma_{cy}A = \sigma_{cy}Wt \qquad \text{(A-1)}$$

Also, the compressive load at buckling would be

$$P_y = \frac{\pi^2 E_t I}{l^2} \qquad \text{(A-2)}$$

For the case of rectangular cross-sections, $I = Wt^3/12$, so that Eq. (2) becomes

$$P_y = \frac{\pi^2 E_t Wt^3}{12l^2} \qquad \text{(A-3)}$$

Combining (A-1) and (A-3) and solving for l,

$$l = \left(\frac{\pi^2 E_t t^2}{12\sigma_{cy}}\right)^{\frac{1}{2}} \qquad \text{(A-4)}$$

Considering the potential energy $(1/2\ K\Delta^2)$ and work $[(2P_{cr}\Delta^2)/l]$, at buckling,

$$K = \frac{4P_{cr}}{l} \qquad \text{(A-5)}$$

Considering the equilibrium condition as shown in Fig. (A-1),

$$P_x = \frac{2\Delta P_y}{l} \qquad \text{(A-6)}$$

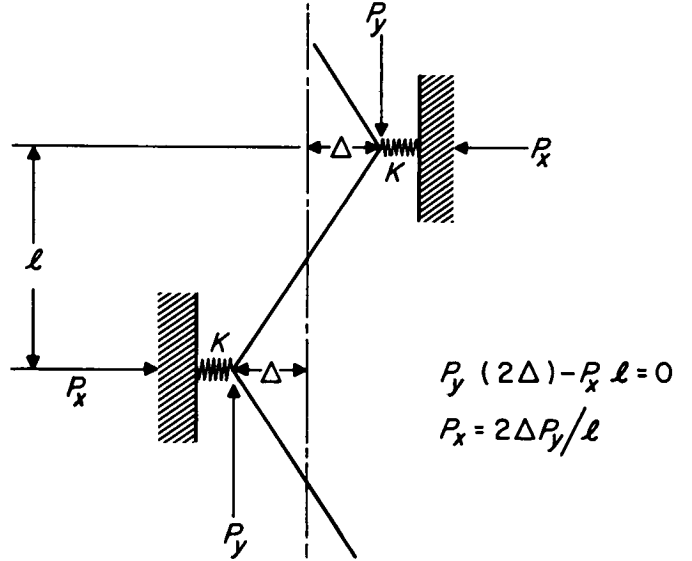$$P_y\,(2\Delta) - P_x\,l = 0$$
$$P_x = 2\Delta P_y / l$$

Figure A-1. Equilibrium-condition diagram

in one member. For a hinged-roller combination, $\Delta = \Delta_0 + 2P_x/K$, so that Eq. (A-6) becomes

$$P_x = \frac{2\left(\Delta_0 + \dfrac{2P_x}{K}\right)P_y}{l} \qquad \text{(A-7)}$$

Solving for P_x and taking $P_{cr} = Kl/4$ from Eq. (A-5),

$$P_x = \frac{\dfrac{2\Delta_0 P_y}{l}}{1 - \dfrac{P_y}{P_{cr}}} \qquad \text{(A-8)}$$

Nomenclature

A area of gage section

E_t tangent modulus

I moment of inertia

K spring constant

l critical wavelength

P_{cr} critical buckling load

P_x lateral load

P_y compressive load

t thickness of gage section

W width of gage section

Δ deflection

Δ_0 eccentricity

σ_{cy} compressive yield strength

ACKNOWLEDGMENTS